

# Trident-type Tuning Fork Silicon Gyroscope by The Phase Difference Detection

Munemitsu Abe, Eiji Shinohara, Kazuo Hasegawa

Shinji Murata, Masayoshi Esashi\*

ALPS ELECTRIC CO., LTD.

\* TOHOKU University

3-31, Akedori, Izumi-ku, Sendai, Japan

E-mail : abemune@gw4.alps.co.jp

\*Aramaki Aza Aoba, Aoba-ku, Sendai, Japan

## ABSTRACT

The trident-type tuning fork silicon gyroscope was designed and fabricated. The trident-type tuning fork structure and vacuum packaging has higher Q value than 15000. A new detection principle which is based on the phase difference detection is proposed and is confirmed using the fabricated gyroscope. By this detecting method, it is possible to detect the angular rate without control of the driving amplitude. Gyroscope sensitivity obtained was  $180 \mu\text{V}/\text{deg}/\text{sec}$ .

## INTRODUCTION

Recently, different type gyroscopes have been developed using silicon micromachining[1] [2] [3]. Most of them are vibrating type gyroscopes. Cantilever type and two tuning fork type were already reported[4] [5], while our structure is the trident-type tuning fork shown in Fig.1.

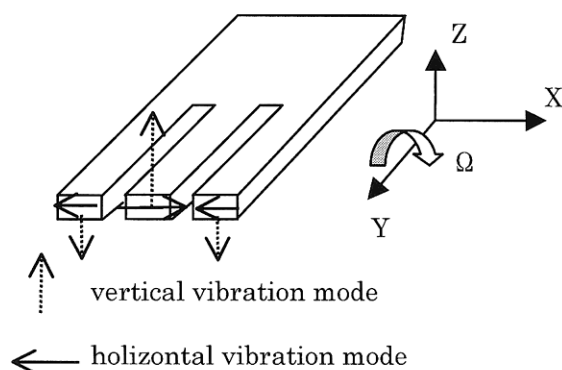


Fig.1 Trident-type tuning fork

The center arm vibration has twice amplitude and out of phase to the other two arms in both

vertical and horizontal directions. As a result, both the vertical vibration and the horizontal vibration are balanced in the trident-type tuning fork, so the energy loss of the vibration is quite small compared with other tuning forks [6]. Hence, both the vertical Q and horizontal Q can be high. The purpose of this work is to develop the trident-type tuning fork silicon gyroscope based on this advantage. Constant driving amplitude is essential for vibrating gyroscope in general, however we developed a new detection method in which detected signal of the angular rate does not depend on the driving amplitude but the ratio of the detected amplitude to the driving amplitude.

## SENSOR STRUCTURE & WORKING PRINCIPLE

The gyroscope structure is shown in Fig2. It consists of glass / silicon / glass packaged structure[7] which has vacuum cavity in it. The thickness of the silicon is 0.2 mm and that of the glass is 0.3mm. The chip size is  $4.0\text{mm} \times 13.6\text{mm} \times 0.8\text{mm}$ . The width and the thickness and the length of all arms are  $200 \mu\text{m} \times 200 \mu\text{m} \times 5800 \mu\text{m}$ . The gaps between the arms and the glasses are  $10 \mu\text{m}$ . On the top and the bottom glasses, driving electrodes and detecting electrodes are formed.

Working principle of the gyroscope is as follows. The tuning fork is driven in Z direction electrostatically. When the angular rate works around the Y-axis, the Coriolis force generate the vibration in X direction and it is detected capacitively.

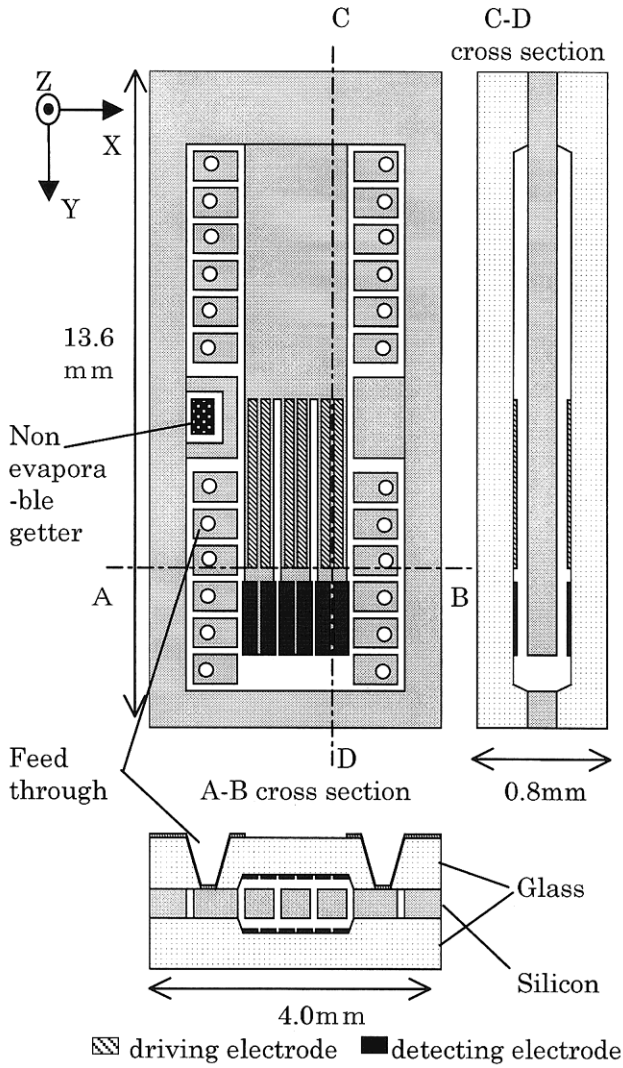


Fig.2 Structure of the gyroscope chip

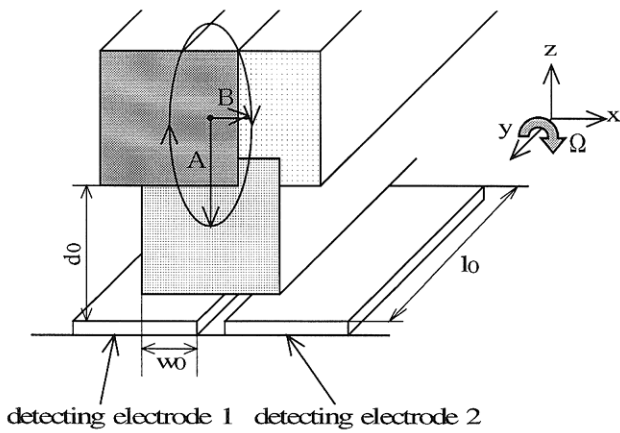


Fig.3 Principle of the phase difference detection

The principle of the phase difference detection is shown in Fig3. The angular rate is detected by the phase difference between the two capacitances obtained with the detecting electrode 1 and 2. The equation of the driving vibration is as follows.  $A$  is the driving amplitude.

$$Z = A \sin \omega t \text{-----(1)}$$

When the angular rate works around the  $Y$ -axis, the Coriolis force  $F$  in equation (2) is caused in  $X$  direction.  $m$  is the equivalent mass of tuning fork and  $\Omega$  is the angular rate.

$$F = 2m \Omega (dZ/dt) \text{-----(2)}$$

Then, the vibration expressed in equation (3) and (4) is generated.  $B$  is the amplitude in  $X$  direction (detecting direction).  $G$  is the coefficient which depends on  $\omega$  (driving frequency),  $\omega_0$  (resonance frequency in  $X$  direction) and  $Q_x$  ( $Q$  value in  $X$  direction) [8].

$$X = B \cos \omega t \text{-----(3)}$$

$$B = A \Omega G \text{-----(4)}$$

The capacitances of the detecting electrode 1 and 2 are

$$C_1(t) = \epsilon_0 l_0 (W_0 + B \cos \omega t) / (d_0 - A \sin \omega t) \text{-----(5)}$$

$$C_2(t) = \epsilon_0 l_0 (W_0 - B \cos \omega t) / (d_0 - A \sin \omega t) \text{-----(6)}$$

$\epsilon_0$ ,  $l_0$ ,  $W_0$ ,  $d_0$  are permittivity in vacuum, the length of detecting electrode, the overlap length between the arm and the detecting electrode and the gap between the arm and the detecting electrode, respectively. The variation of the  $C_1(t)$ ,  $C_2(t)$  are shown in Fig.4.

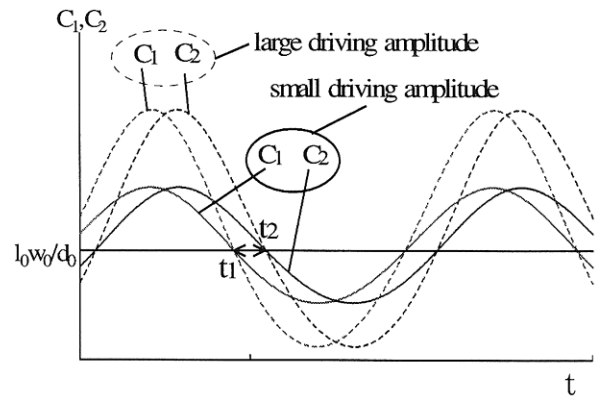


Fig.4 Simulation result

When  $C_1(t_1) = C_2(t_2) = \varepsilon_0 l_0 W_0 / d_0$ , following equations are given from equations (5) and (6).

$$t_1 = -\tan^{-1}\{(B/W_0)/(A/d_0)\} \text{-----(7)}$$

$$t_2 = \tan^{-1}\{(B/W_0)/(A/d_0)\} \text{-----(8)}$$

In the condition of  $(B/W_0)/(A/d_0) \div 0$ , we obtain equation (9) from equation (4)

$$t_2 - t_1 \approx 2(B/W_0)/(A/d_0) = 2(Gd_0/W_0) \Omega \text{-----(9)}$$

The angular rate  $\Omega$  is detected as a phase difference obtained from “ $t_2 - t_1$ ”. Because the coefficient  $Gd_0/W_0$  in equation (9) does not depend on the driving amplitude  $A$ , it is not necessary to control the driving amplitude in this phase difference detection. The simulation result is shown in Fig.4.

## PROCESS

The process flow of the gyroscope is shown in Fig.5.

### Bottom glass process (A)

- (A1) Glass etching in 50% HF using resist and chromium as a mask.
- (A2) Metalization(Pt/Ti) and patterning for driving and detecting electrodes.

### Top glass process (B)

- (B1) Forming feed through holes in glass by sand brust.
- (B2) and (B3) are the same as (A1), (A2).

### Silicon process (C)

- (C1) Anodic bonding of a silicon and the bottom glass in vacuum.
- (C2) Silicon etching by ICP-RIE(Inductive Coupling Plasma – Reactive Ion Etching) [9] to form the tuning fork.
- (C3) Anodic bonding to the top glass in vacuum for vacuum sealing in which the non evaporable getter is used [10]. Vacuum cavity is required to prevent the viscous dumping of the resonator.
- (C4) Metalization(Au/Cr) and patterning for outer lead.

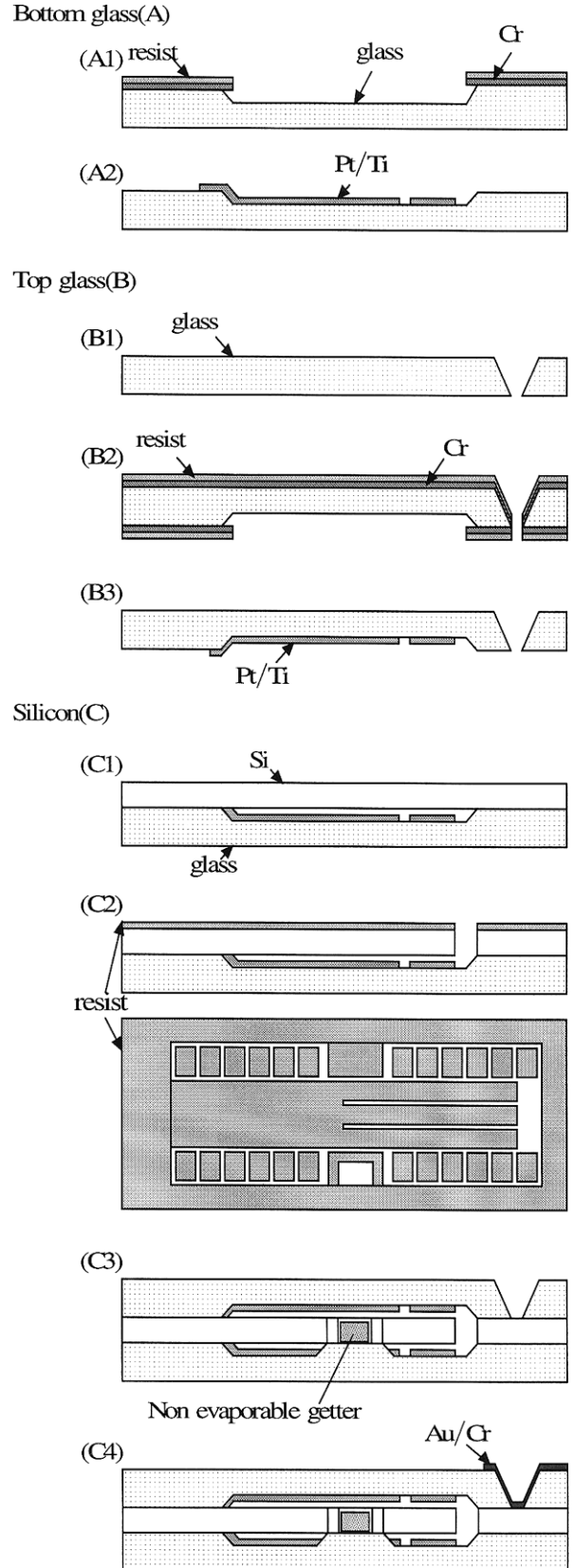


Fig.5 Process flow of gyroscope

The SEM photographs of the fabricated tuning fork are shown in Fig.6 and Fig.7. The photograph of the chip is shown in Fig.8.

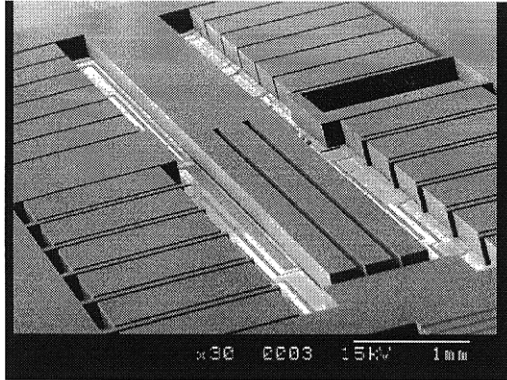


Fig.6 SEM photograph of gyroscope

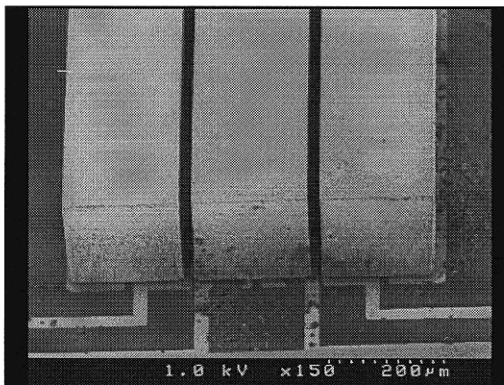


Fig.7 SEM photograph of tuning fork

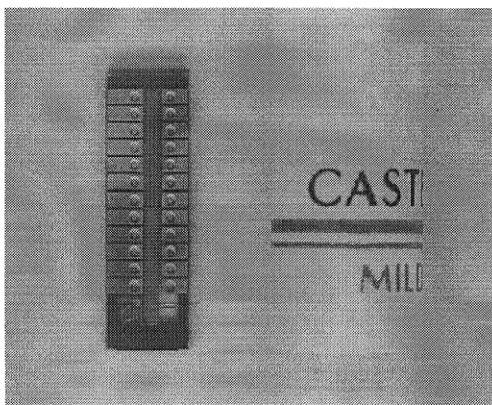


Fig.8 Photograph of chip

## MESUREMENT OF THE VIBRATION MODE OF TRIDENT-TYPE TUNING FORK

The resonance characteristics are measured by the laser doppler vibrometer. The driving voltage is applied to the center arm and the other two arms alternatively. The resonance characteristics in Z axis direction are shown in Fig.9-1, Fig.9-2, Fig.9-3. The phase difference was 180 degree between the center arm and the other two arms, and this confirms the expected vibration mode of the trident-type tuning fork.

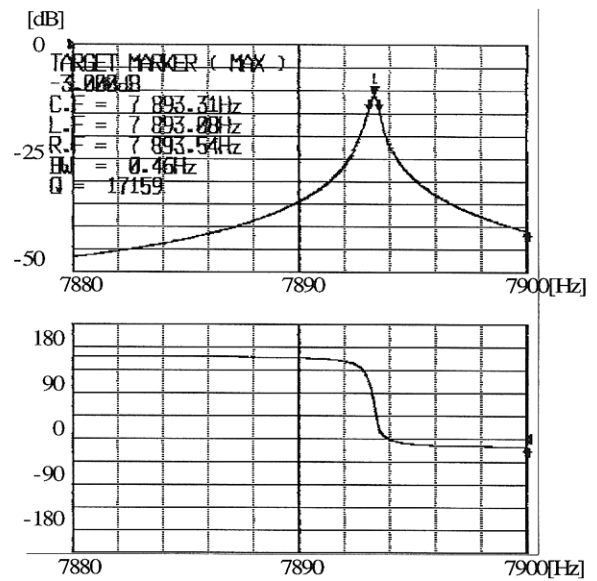


Fig.9-1 Vibration of center arm

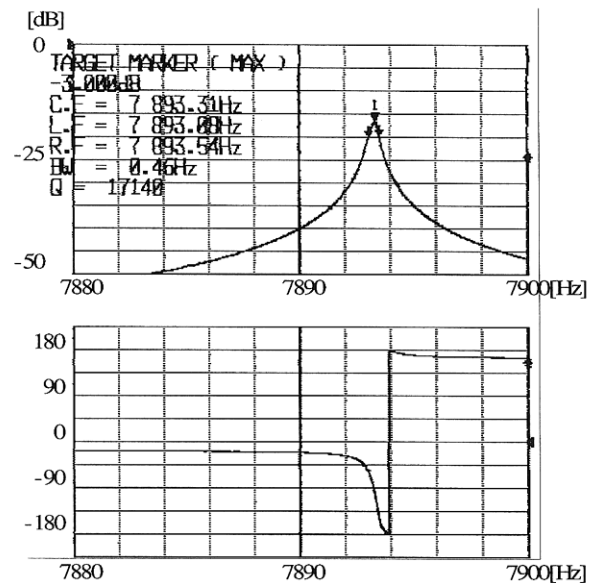


Fig.9-2 Vibration of right arm

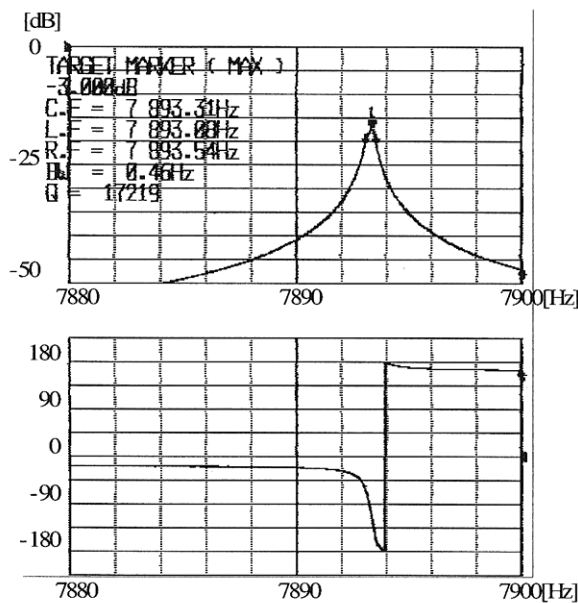


Fig.9-3 Vibration of left arm

### CHARACTERIZATION OF THE VIBRATION

The pressure dependency of the resonance frequency, Q value, amplitude in Z axis direction are shown in Fig10-1, Fig10-2, Fig10-3. Resonance frequency is independent of pressure (Fig10-1). The higher Q value than 15000 is achieved at low pressure less than 1Pa.(Fig10-2). The amplitude of the center arm is twice those of the other two arms(Fig10-3).

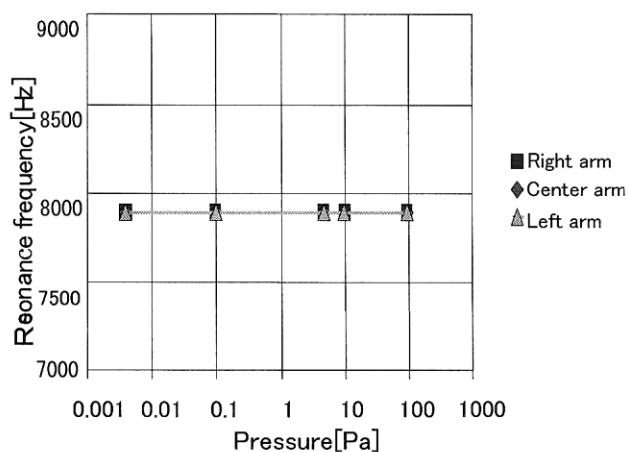


Fig.10-1 Resonance frequency vs Pressure

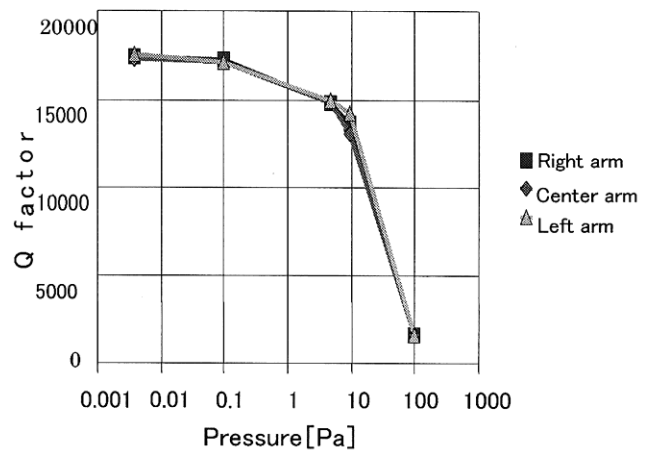


Fig.10-2 Q value vs Pressure

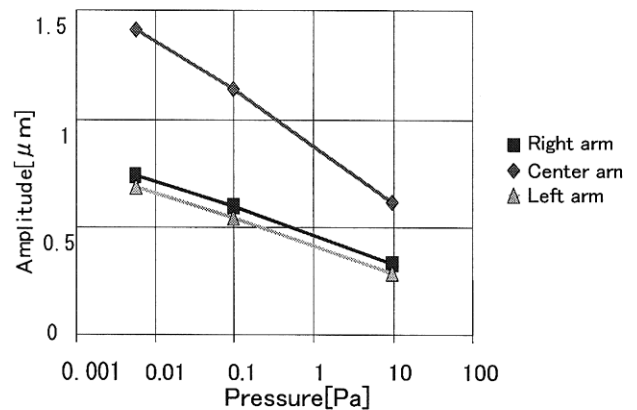


Fig.10-3 Driving amplitude vs Pressure

### EVALUATION AS A GYROSCOPE

The gyroscope was driven with 2Vpp at the resonance frequency of 7893 Hz. The pressure in the vacuum sealed cavity was 0.1 Pa. The excitation amplitude was 1.2  $\mu m$ . The circuit to evaluate the gyroscope is shown in Fig.11. The angular rate was measured in the range of  $\pm 280$  degree. The sensitivity of the gyroscope was 180  $\mu V/deg/sec$ .

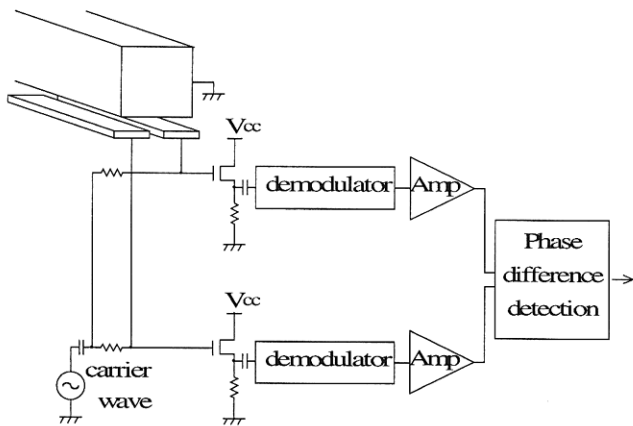


Fig.11 Circuit to evaluate the gyroscope

## CONCLUSION

The trident-type tuning fork silicon gyroscope was designed and fabricated. The new detection method which is based on the phase difference detection is proposed and confirmed using the fabricated gyroscope. This method is able to detect the angular rate without the control of the driving amplitude. This detecting method is able to be applied to the other vibrating gyroscopes.

## ACKNOWLEDGMENTS

This work is supported by Japanese Ministry of Education Science and Culture under a Grant-in-Aid No.10305033.

## REFERENCE

- [1]J.Choi, R.Toda, M.Esashi, "Silicon Angular Resonance Gyroscope By Deep ICPRIE AND XeF<sub>2</sub> GAS Etching." Micro Electro Mechanical Systems (1998). pp.322-327.
- [2]S.S.Baek, Y.S.Oh, B.J.Ha, "A Symmetrical Z-Axis Gyroscope With A High Aspect Ratio Using Simple And New Process." Micro Electro Mechanical Systems (1999). pp.612-617.
- [3]K.Funk, H.emmerrich, A.Schilp, " A Surface Micromachined Silicon Gyroscope Using A Thick Polysilicon Layer". Micro Electro Mechanical Systems (1999). pp.57-60.
- [4]K.Maenaka,T.Shiozawa. "A study of silicon angular rate sensors using anisotropic etching Technology", Sensors and Actuators A.43 (1994) pp.72-77.
- [5] S.Sassen, R.Voss, "Silicon Angular Rate Sensor for Automotive Applications with Piezoelectric Drive and Piezoresistive Read-Out". Transducers '99,(1999) pp.906-909.
- [6]A.Satoh, Y.Tomikawa,and K.Ohnishi, "Piezoelectric Vibratory Gyro Sensor Using a Trident-Type Tuning Fork Resonator", Jpn. J. Appl. Phys, Vol.33, Pt.1, No.9B, pp.5361-5364(1994)
- [7]M.Esashi, "Encapsulated micro mechanical sensors" . Microsystem technologies 1(1994)pp2-9.
- [8]K.Maenaka, T.Fujita, M.Maeda, "Design Problems on Vibratory Micro-Gyroscopes." The Transactions of The Institute of Electrical Engineers of Japan Vol.118—E, No7/8, (1998) pp377-383.
- [9]A.M.Hynes, H.Ashraf, J.K.Bhardwaj, "Recent Advances in silicon etching for MEMS using the ASE™ process". Sensors and Actuators A, 74 (1999) pp13-17
- [10]H.Henmi, S.Shoji, M.Esashi, "Vacume Packaging For Microsensors By Glass-Silicon Anodic Bonding". Sensors and Actuators A, 43(1994) pp243-248